Clathrin phosphorylation is required for actin recruitment at sites of bacterial adhesion and internalization

Matteo Bonazzi,[1,2,3] Lavanya Vasudevan,[4,5,6] Adeline Mallet,[7] Martin Sachse,[7] Anna Sartori,[7] Marie-Christine Prevost,[7] Allison Roberts,[4,5,6] Sabrina B. Taner,[4,5,6] Jeremy D. Wilbur,[4,5,6] Frances M. Brodsky,[4,5,6] and Pascale Cossart[1,2,3]

[1]Institut Pasteur, Unité des Interactions Bactéries-Cellules, Paris F-75015, France
[2]Inserm, U604, Paris, F-75015 France
[3]Institut National de la Recherche Agronomique, USC2020, Paris F-75015, France
[4]Department of Bioengineering and Therapeutic Sciences, [5]Department of Microbiology and Immunology, and [6]Department of Pharmaceutical Chemistry, The G.W. Hooper Foundation, University of California, San Francisco, San Francisco, CA 94143-0552
[7]Institut Pasteur, Plateforme de Microscopie Ultrastructurale, Imagopole, Paris F-75015, France

Bacterial pathogens recruit clathrin upon interaction with host surface receptors during infection. Here, using three different infection models, we observed that host–pathogen interactions induce tyrosine phosphorylation of clathrin heavy chain. This modification was critical for recruitment of actin at bacteria–host adhesion sites during bacterial internalization or pedestal formation. At the bacterial interface, clathrin assembled to form coated pits of conventional size. Because such structures cannot internalize large particles such as bacteria, we propose that during infection, clathrin-coated pits serve as platforms to initiate actin rearrangements at bacteria–host adhesion sites. We then showed that the clathrin–actin interdependency is initiated by Dab2 and depends on the presence of clathrin light chain and its actin-binding partner Hip1R, and that the fully assembled machinery can recruit Myosin VI. Together, our study highlights a physiological role for clathrin heavy chain phosphorylation and reinforces the increasingly recognized function of clathrin in actin cytoskeletal organization in mammalian cells.

Introduction

Clathrin coats membranes of vesicles formed during receptor-mediated endocytosis and organelle biogenesis from the trans-Golgi network (Brodsky et al., 2001). Clathrin can also form extended lattices with no curvature at cell–substrate interfaces (plaques; Saffarian et al., 2009) and patches on endosomes (Popoff et al., 2009; Raiborg and Stenmark, 2009). The clathrin coat itself is formed by self-assembly of triskelion-shaped molecules composed of three clathrin heavy chains (CHCs) and associated clathrin light chain (CLC) subunits (Brodsky et al., 2001). Clathrin coats form at membranes by binding a variety of adaptor molecules that select the cargo molecules sequestered into the coat for sorting. During internalization of receptors that stimulate Src family kinases, including the receptor tyrosine kinase (RTK) EGF receptor (EGFR) and T and B lymphocyte receptors, CHC is modified by tyrosine phosphorylation (Wilde et al., 1999; Stoddart et al., 2002; Crotzer et al., 2004). The function or molecular details of this modification have not been fully defined, but Src family kinase phosphorylation of CHC is specifically required for uptake of these signaling receptors (Crotzer et al., 2004). Clathrin is also required for the internalization of large objects such as bacteria (Veiga and Cossart, 2005; Veiga et al., 2007; Eto et al., 2008; Chan et al., 2009), fungi hyphae (Moreno-Ruiz et al., 2009), and large viruses (Cureton et al., 2009) in a process that involves cooperation with actin. In the case of *Listeria monocytogenes* (Sousa et al., 2007; Bonazzi et al., 2008), pathogenic adhesion and infection involve signaling through Src family tyrosine kinases triggered

Correspondence to Matteo Bonazzi: matteo.bonazzi@cpbs.cnrs.fr; Frances M. Brodsky: Frances.Brodsky@ucsf.edu; or Pascale Cossart: pcossart@pasteur.fr

Matteo Bonazzi's present address is UMR 5236, Centre d'études d'agents Pathogènes et Biotechnologies pour la Santé (CPBS), Centre National de la Recherche Scientifique, Université Montpellier 1, Université Montpellier 2, 34293 Montpellier, France.

Abbreviations used in this paper: CHC, clathrin heavy chain; CLC, clathrin light chain; EPEC, enteropathogenic *Escherichia coli*; MALDI, matrix-assisted laser desorption/ionization; TOF, time of flight; wt, wild type.

The Rockefeller University Press $30.00
J. Cell Biol. Vol. 195 No. 3 525–536
www.jcb.org/cgi/doi/10.1083/jcb.201105152

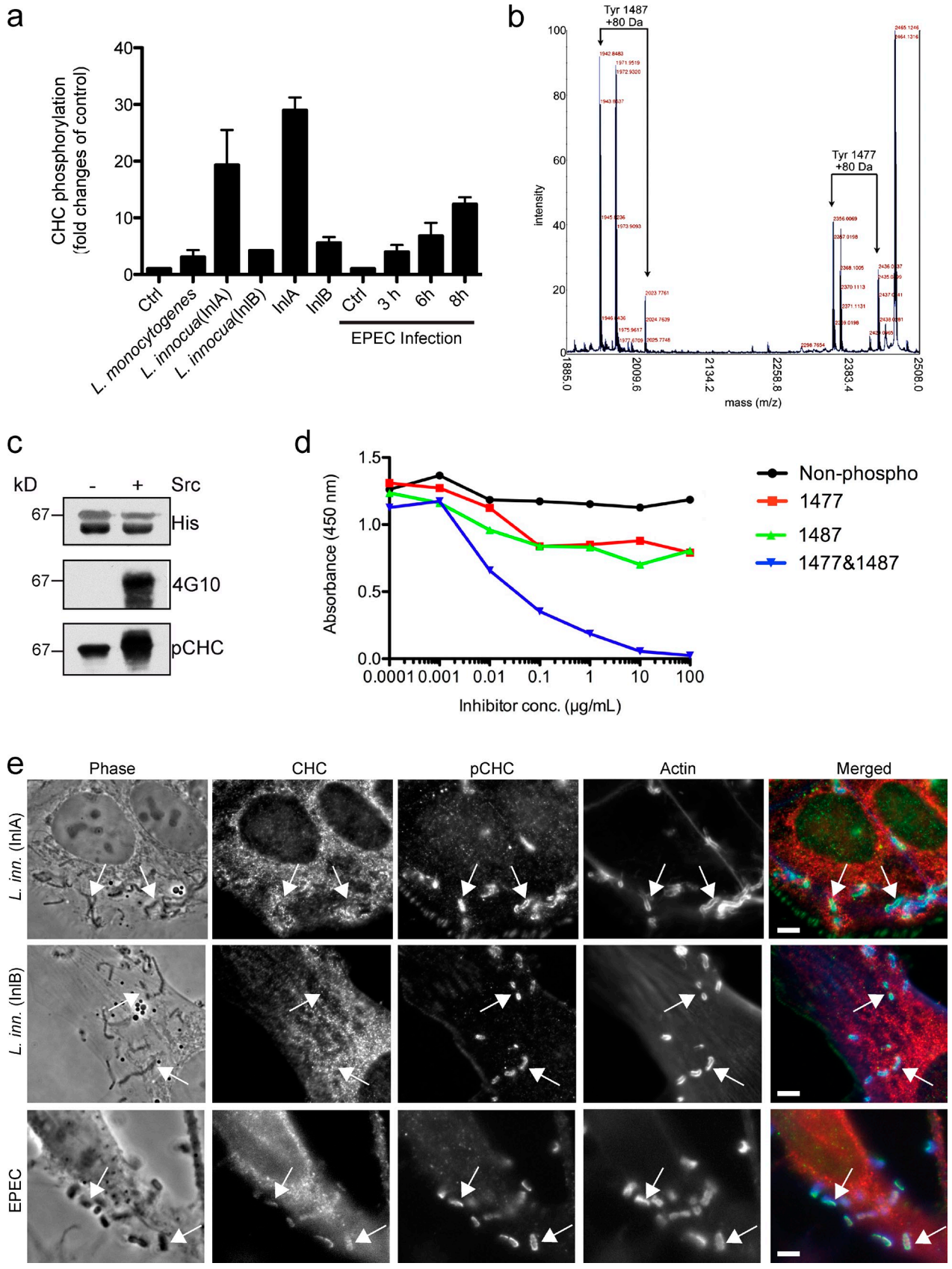

Figure 1. **Infection induces CHC phosphorylation.** (a) Quantification of the intensity of chemiluminescence of three independent Western blots of Jeg3 cells treated as indicated or HeLa cells infected with EPEC for the indicated times. After each treatment, CHC was immunoprecipitated and tyrosine phosphorylation was assayed with the anti-phosphotyrosine antibody PY20. Error bars indicate mean ± SD. (b) MALDI-TOF mass spectrometry spectrum of in vitro phosphorylated CHC fragment (1074–1675). Src kinase was incubated with recombinant CHC followed by digestion with trypsin. Tyr 1487 is

by bacterial binding to host-cell receptors. Similarly to *L. monocytogenes*, enteropathogenic *Escherichia coli* (EPEC) require clathrin during infection, but unlike *L. monocytogenes*, EPEC are not internalized by host cells and form actin-based pedestals at the sites of interaction with the infected cell (Wong et al., 2011). In this study, we address whether Src family kinase-mediated tyrosine phosphorylation of CHC occurs during bacteria–cell interaction and whether the infectious process might reveal a function for CHC phosphorylation in the context of clathrin–actin interactions.

Our understanding of clathrin–cytoskeleton interactions during clathrin-mediated processes is evolving. The participation of clathrin in uptake of pathogens challenges the concept of a size limit for clathrin cargo and implicates clathrin–actin interactions in pathogen internalization pathways (Pizarro-Cerdá et al., 2010). During infection, clathrin and actin accumulate at sites of bacteria–host interactions, and clathrin recruitment precedes actin rearrangements that are critical both for bacterial internalization and for the formation of bacteria-induced actin pedestals (Veiga et al., 2007). These observations coincide with an increasingly recognized connection between clathrin and the actin cytoskeleton in mammalian cells (Merrifield et al., 2002; Yarar et al., 2005; Hyman et al., 2006) that goes beyond colocalization (Ferguson et al., 2009). The two mammalian CLCs (LCa and LCb) both interact with actin-binding proteins Hip1 and Hip1R via a shared 22–amino acid sequence in their N terminus (Chen and Brodsky, 2005; Legendre-Guillemin et al., 2005). Binding of CLCs to Hip proteins regulates their interaction with actin and affects actin dynamics (Engqvist-Goldstein et al., 2001; Engqvist-Goldstein et al., 2004; Wilbur et al., 2008). The importance of a functional link between clathrin and actin, via the CLC–Hip interaction, has been well-established in yeast, where the Hip homologue Sla2p is essential for clathrin-mediated endocytosis (Newpher and Lemmon, 2006); its role in various forms of mammalian cell endocytosis is still being defined (Kaksonen et al., 2006; Saffarian et al., 2009). Actin is present at clathrin plaques, which requires CLC–Hip interaction, and is also situated where the neck of a clathrin-coated pit elongates, apparently directing coated vesicles away from the plasma membrane (Collins et al., 2011). This latter activity is needed for coated vesicles to form at membranes with high surface tension (Boulant et al., 2011). The molecular details of how clathrin and actin coordinate during bacterial interaction with the host cell surface are defined in the investigation reported here.

By analysis of clathrin coat formation, the role of clathrin phosphorylation, and the interaction of clathrin with actin during bacteria–host cell attachment and internalization, we establish the sequence of molecular events during early stages of infection. We show that bacteria–host adhesion involves the adaptor Dab2 to form clathrin-coated pits that support actin recruitment via CLC and Hip1R. The motor protein Myosin VI is then recruited to provide a pulling force for bacterial internalization. Moreover, we show that, similar to the endocytosis of signaling receptors, the phosphorylation of CHC is triggered by bacterial infection and that this modification is critical for effective function of the clathrin platform as an actin organizer during bacterial internalization and pedestal formation.

Results

CHC phosphorylation is required for bacterial internalization or pedestal formation

Signaling through tyrosine kinases promotes the localization of clathrin at the plasma membrane, dependent on tyrosine phosphorylation of CHC (Wilde et al., 1999; Crotzer et al., 2004). This phosphorylation is mediated by Src family kinases (Src, Lyn, or Lck; Wilde et al., 1999; Stoddart et al., 2002; Crotzer et al., 2004). The same kinases are also activated during the clathrin-dependent internalization of *L. monocytogenes* by the InlA pathway (Sousa et al., 2007; Veiga et al., 2007; Bonazzi et al., 2008). We therefore tested the possibility that bacteria, which use clathrin to invade host cells (Veiga et al., 2007), trigger the phosphorylation of CHC. Epithelial cells were incubated for 1 h with either *L. monocytogenes*, or with the noninvasive strain *Listeria innocua* expressing either one of the two *Listeria* invasion proteins InlA or InlB (*L. innocua*(InlA) and *L. innocua*(InlB)) to specifically follow the two internalization pathways used by *Listeria* during infection (Jonquières et al., 1999; Sousa et al., 2007; Veiga et al., 2007; Bonazzi et al., 2008). Alternatively, HeLa cells were infected with EPEC for 3, 6, and 8 h. In addition, to directly test the possibility that bacterial signaling is involved in CHC phosphorylation, cells were also incubated with either purified InlA or InlB for 1 h. CHC was then immunoprecipitated and tyrosine phosphorylation was analyzed by Western blotting. In all cases, we could detect a significant degree of CHC phosphorylation (Fig. 1 a and Fig. S1, a and b), with the strongest phosphorylation of CHC upon exposure to InlA and

found within a peptide with a predicted monoisotopic mass of 1942.9 D and within the phosphopeptide with a predicted mass of 2022.9 D. Tyr 1477 is found within a peptide with a predicted monoisotopic mass of 2355.1 D and within the phosphopeptide with a predicted mass of 2435.1 D. Arrows indicate the native and phosphorylated peptides. (c) Purified recombinant his-tagged-hub fragment of CHC (residues 1074–1675) was treated with or without recombinantly purified Src kinase for 3 h at room temperature. Samples were immunoblotted with antibody against the histidine tag on the hub (His, as loading control), 4G10 (for phospho-tyrosine), and anti-phospho-CHC antibody (pCHC) purified by affinity column and by membrane-based depletion. (d) Anti-pCHC (affinity purified by column) was tested for binding to the 1477&1487-phospho-peptide in the presence of the nonphospho-peptide, 1477-phospho-peptide, 1487-phospho-peptide, or 1477&1487-phospho-peptide at the indicated dilutions by ELISA. (e) Jeg3 cells were infected with *L. innocua*(InlA) for 30 min and HeLa cells were infected with *L. innocua*(InlB) for 5 min or with EPEC for 6 h. After infections, cells were fixed and labeled for total CHC (CHC, red) and phospho-CHC (pCHC, green), and F-actin was labeled with fluorescent phalloidin (actin, blue). Arrows indicate colocalization between bacteria, pCHC, and actin. Bars 10 µm.

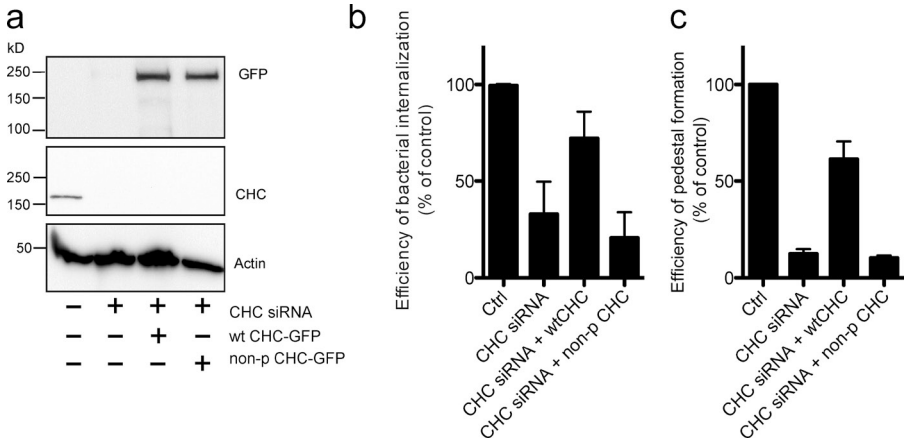

Figure 2. **CHC phosphorylation is required for bacterial infection and pedestal formation.** (a) Representative Western blot of Jeg3 cells transfected with a control siRNA or with a CHC-targeted siRNA alone or in combination with the overexpression of wt CHC-GFP or the Y1477, 1487F mutant of CHC-GFP (non-pCHC-GFP). Comparable results were obtained in HeLa cells. Note that the GFP tag on the rescue constructs interferes with reactivity of the TD.1 antibody against the CHC N-terminal domain (Näthke et al., 1992) used for immunoblotting. (b and c) Jeg3 cells and HeLa cells were then infected with *L. monocytogenes* and HeLa cells with EPEC. Bacterial internalization and EPEC pedestal formation were quantified by immunofluorescence. In all cases, values are means ± SD of three independent experiments (error bars).

after 8 h of EPEC infection (Fig. 1 a). Because Src is activated during the InlA-mediated internalization of *L. monocytogenes*, we tested the possibility that, at least in this pathway, Src mediates CHC phosphorylation. Indeed, treatment of Jeg3 cells with the Src family kinase inhibitor PP1, before InlA binding, totally prevented CHC phosphorylation (Fig. S1 c).

We previously identified CHC tyrosine 1477 as a target site for Src family kinases by peptide mapping and mutagenesis (Wilde et al., 1999). Further mass spectrometry analysis of the purified recombinant hub fragment of clathrin (residues 1,074–1,675) incubated with purified Src kinase revealed that tyrosine 1487 is also a target phosphorylation site (Fig. 1 b). To be able to specifically identify phosphorylated clathrin in vivo, we raised a polyclonal antibody against a phospho-peptide comprising these two target sites (anti-pCHC). This antibody was purified by depletion with nonphosphorylated peptide, followed by affinity purification with the 1477&1487-phospho-peptide. Western blotting showed a preferential affinity of this antibody for Src-phosphorylated clathrin hub fragment compared with unphosphorylated hub (Fig. 1 c). By inhibition of antibody binding to the 1477&1487-phospho-peptide with nonphospho-peptide or peptides phosphorylated only at 1477 or 1487 or the 1477&1487-phospho-peptide, the affinity-purified antibody was shown to primarily recognize an epitope dependent on phosphorylation of both target sites (Fig. 1 d). The anti-pCHC had minimal reactivity with peptides phosphorylated at each single site or the nonphospho-peptide. Analysis of cells stimulated with EGF showed that the anti-pCHC recognized the plasma membrane clathrin that accumulates upon EGF signaling and did not detect the intracellular clathrin recognized by the X22 monoclonal antibody (Fig. S2; Brodsky, 1985).

The anti-pCHC antibody was then used to label cells during infection. In addition, F-actin was labeled by fluorescent phalloidin. Jeg3 cells were infected with *L. innocua*(InlA) for 30 min and HeLa cells were infected with *L. innocua*(InlB) or with EPEC for 5 min or 6 h, respectively. In all three cases, phospho-CHC was highly enriched around all bacteria that recruited F-actin, and the intracellular staining of phospho-CHC was negligible (Fig. 1 d). In contrast, as previously reported (Veiga and Cossart, 2005), the X22 antibody against total CHC labeled cytosolic structures as well as bacteria cell adhesion sites (Fig. 1 d).

We next tested the role of the CHC phosphorylation in *Listeria* internalization and in the formation of EPEC-induced actin pedestal. To do so, endogenous CHC was depleted by siRNA in Jeg3 and HeLa cells, and CHC expression was rescued by transfecting with either wild-type (wt) CHC-GFP or a mutant CHC-GFP with tyrosines 1477 and 1487 changed to phenylalanines (Y1477, 1487F). Both constructs carried point mutations to avoid siRNA sensitivity (Fig. 2 a). Jeg3 and HeLa cells were then infected with *L. monocytogenes* or with EPEC, respectively. Bacterial internalization was evaluated by differential immuno-labeling, and actin-based pedestals were quantified by labeling F-actin with fluorescent phalloidin. As previously reported (Veiga et al., 2007), clathrin depletion inhibited both *Listeria* internalization and EPEC pedestal formation (Fig. 2, b and c). Strikingly, the expression of wt CHC-GFP restored bacterial entry and pedestal formation to ∼70% and 60% of control cells, respectively, whereas the expression of the Y1477, 1487F mutant CHC-GFP failed to do so (Fig. 2, b and c), establishing that CHC phosphorylation is critical for efficient *L. monocytogenes* internalization and EPEC pedestal formation.

Ultrastructural analysis of clathrin recruitment at bacterial adhesion and entry sites

Since our first study of a role for clathrin in bacterial internalization, a key issue has been to explain how structures that do not normally exceed a diameter >200 nm can mediate the internalization of much larger particles such as bacteria and fungus hyphae (Veiga and Cossart, 2005; Veiga et al., 2007; Moreno-Ruiz et al., 2009). The optical resolution of conventional fluorescence microscopy is not sufficient to determine whether clathrin accumulation during infection corresponds to the formation of a homogeneous coat, of multiple coated pits, or represents the recruitment of clathrin-coated vesicles from other intracellular compartments. Here we investigated the ultrastructural organization of clathrin at the *Listeria* entry sites and at enteropathogenic *E. coli* (EPEC)-induced actin pedestals by electron microscopy. To study *Listeria* uptake, cells were infected with either *L. innocua* (InlA) or *L. innocua*(InlB) for 15 and 30 min. From previous studies, these correspond to the time points when clathrin was more frequently observed at *Listeria*

entry sites. By electron microscopy, we never observed homogeneous clathrin coats around invading bacteria, but rather only isolated clathrin-coated pits, with a size similar to that previously reported in literature (Fig. 3, a–c). To test the possibility that clathrin might form atypical coats at bacteria, clathrin localization was also established by immuno-labeling of thawed cryosections from HeLa cells infected with *L. monocytogenes*. Confirming our morphological analysis, clathrin labeling was never observed on flat membrane surfaces surrounding the bacteria, but always in association with membranous invaginations (Fig. 3 d). These results confirm previous early observations from our laboratory showing the presence of isolated clathrin-coated pits that formed at the *Listeria* entry site (Mengaud et al., 1996). The observation of clathrin at membrane invaginations suggests that bacteria trigger the formation of clathrin-coated pits rather than the recruitment of clathrin-coated vesicles. Furthermore, complete clathrin-coated vesicles were rarely observed in the vicinity of the bacterial entry sites, which suggests the presence of stable clathrin-coated pits, rather than active zones of endocytosis.

As the size of the observed clathrin-coated pits was incompatible with that of bacteria, we hypothesized that during infection, clathrin may serve a different role rather than that of a vesicle coat protein for endocytosis. Our hypothesis was further strengthened by the study of EPEC infection. We previously found that during EPEC infections, clathrin depletion impairs actin recruitment to bacterial adhesion sites, therefore blocking the formation of pedestals (Veiga et al., 2007). Interestingly, our electron microscopy analysis showed that clathrin also appeared as coated pits, but not vesicles, at EPEC-induced actin pedestals (Fig. 3 e). As clathrin is required for actin recruitment during bacterial internalization and EPEC-induced pedestal formation, we suggest that, during infection, stable clathrin-coated pits may serve as a platform for cytoskeletal rearrangements.

We next tested the possibility that clathrin recruitment by bacteria during infection affects conventional clathrin-mediated endocytosis. Jeg3 cells were preincubated with Cy3-labeled transferrin for 30 min on ice, and transferrin was chased for 1 h at 37°C in noninfected as well as in *L. innocua*(InlA)-, *L. innocua*(InlB)-, and EPEC-infected cells. Cells were then acid washed before fixation to remove cell surface–bound transferrin, and the efficiency of transferrin internalization was assessed by fluorescence microscopy. Infected cells were able to internalize transferrin as efficiently as noninfected cells (Fig. S3), which indicates that bacterial entry has no general effect on the overall active cycle of clathrin coat assembly and disassembly.

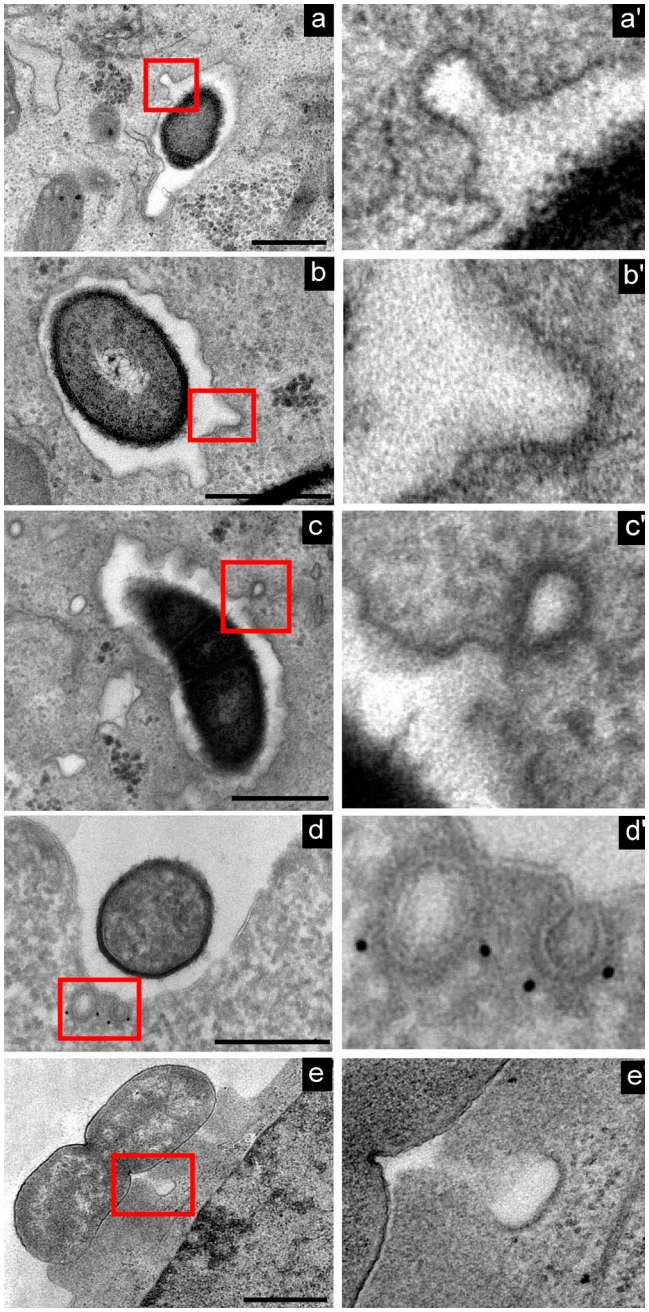

Figure 3. **Ultrastructure of clathrin coats during bacterial infections.** (a–c and e) Jeg3 cells were incubated with *L. innocua*(InlA) (a and b) and HeLa cells with *L. innocua*(InlB) (c) or EPEC (e), fixed, and processed for electron microscopy. (d) HeLa cells were infected with *L. monocytogenes* and processed for immuno-labeling on thawed cryosections where clathrin was localized by antibody labeling. Enlarged views of the boxed regions are shown on the right. Bars, 1 µm.

Dab2, Myosin VI, and Hip1R orchestrate actin association with clathrin coats

We previously found that *L. monocytogenes* infections by the InlA–E-cadherin or the InlB–Met internalization pathways as well as EPEC infections require clathrin coat formation upstream of the rearrangements of the actin cytoskeleton that result from host–pathogen interactions (Veiga and Cossart, 2005; Veiga et al., 2007). To investigate these observations further, we infected HeLa cells with *L. innocua*(InlB) or EPEC and Jeg3 cells with *L. innocua*(InlA), and used a candidate-based approach to investigate the molecular machinery that connects actin dynamics with clathrin coats. Cells were infected with *L. innocua*(InlA) or *L. innocua*(InlB) for 15, 30, and 45 min, and EPEC infections were performed for 4, 5, and 6 h. These time points correspond to the maximal frequency of clathrin recruitment during infection. As the identification of the clathrin adaptor involved in *L. monocytogenes* internalization remains elusive (Veiga and Cossart, 2005; Pizarro-Cerdá et al., 2007),

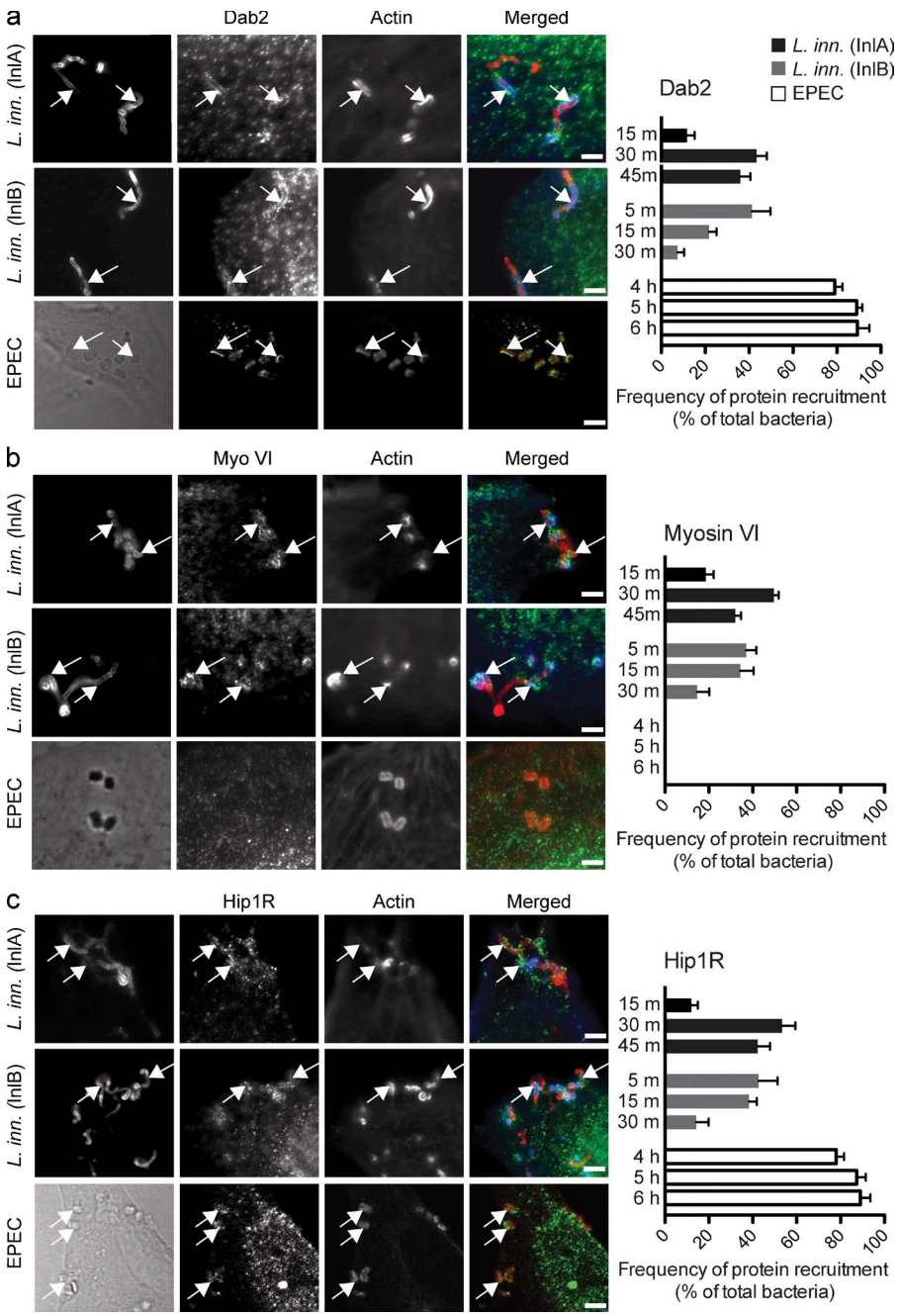

Figure 4. **Recruitment of actin-organizing machinery during infection.** Jeg3 cells were incubated with *L. innocua*(InlA, red) for 15, 30, and 45 min, and HeLa cells were incubated with *L. innocua*(InlB, red) for 5, 15, and 30 min or with EPEC for 4, 5, and 6 h, then fixed and processed for immunofluorescence with antibodies recognizing Dab2, myosin VI, or Hip1R (all green). Actin was labeled with fluorescent phalloidin (blue). At each time point of infection, the frequency of protein recruitment at bacteria adhesion sites was evaluated by immunofluorescence. Arrows point to sites of colocalization between bacteria, the labeled protein, and actin. Values are means (±SD) of three independent experiments where 100 bacteria were counted for each condition. Error bars indicate mean ± SD. Bars, 10 µm.

we first studied Dab2, a nonclassical clathrin adaptor that has recently been associated with the formation of unusually large clathrin lattices at the plasma membrane (Mettlen et al., 2010). Dab2 localized, together with actin, at the entry site of both *L. innocua*(InlA) and *L. innocua*(InlB), with a higher frequency of protein recruitment at 30 and 15 min, respectively (Fig. 4 a). Dab2 was also present at the interface between EPEC and actin pedestals throughout the 4–6-h period observed (Fig. 4 a).

In addition to its role as a clathrin adaptor, Dab2 regulates clathrin-mediated endocytosis by interacting with the molecular motor Myosin VI (Inoue et al., 2002; Morris et al., 2002), which drives the internalization of clathrin-coated vesicles by moving toward the minus end of actin cables (Buss et al., 2001a,b). In our infection models, the localization of Myosin VI coincided with Dab2 at the *Listeria* entry sites, but interestingly, we could never observe the accumulation of Myosin VI at EPEC-induced actin-based pedestals (Fig. 4 b). We then investigated the recruitment of Hip1R, a key player in actin dynamics at clathrin coats (Engqvist-Goldstein et al., 2001; Carreno et al., 2004; Engqvist-Goldstein et al., 2004; Chen and Brodsky, 2005; Newpher and Lemmon, 2006; Le Clainche et al., 2007; Wilbur et al., 2008), as well as a component of clathrin-coated plaques (Saffarian et al., 2009). Hip1R colocalized with actin at sites of *L. innocua*(InlA) and *L. innocua*(InlB) infection by both the InlA–E-cadherin and the InlB–Met entry pathways, and at the interface between EPEC and the actin-based pedestals (Fig. 4 c). Also in this case, the frequency of Hip1R recruitment was maximal at 30 min of infection with *L. innocua*(InlA) and

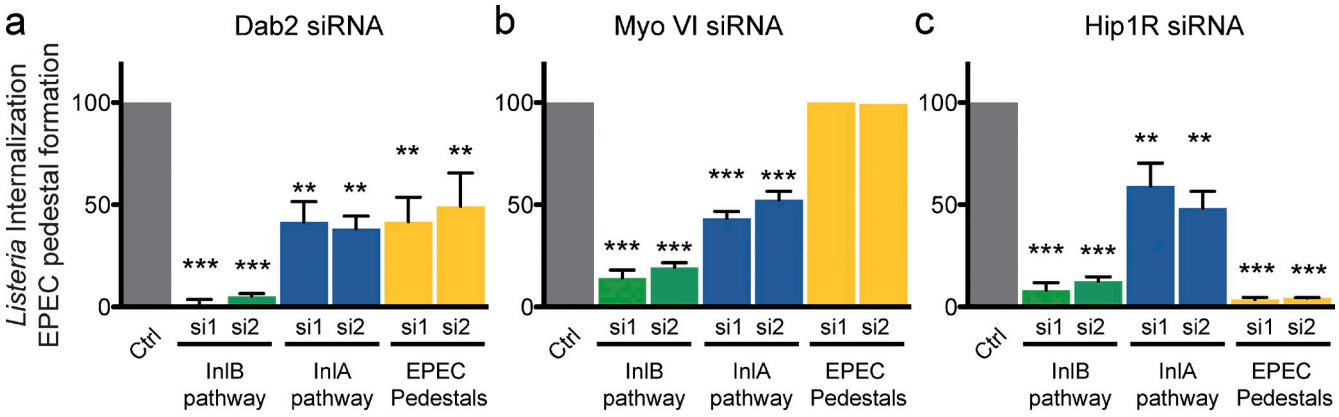

Figure 5. **Dab2, Myosin VI, and Hip1R are required during bacterial infections.** (a–c) Jeg3 cells and HeLa cells were transfected with two siRNA sequences (si1 and si2) targeted to Dab2 (a), Myosin VI (b), or Hip1R (c). *L. monocytogenes* was then used to infect Jeg3 and HeLa cells to follow the InlA or InlB internalization pathway, respectively, by a gentamicin survival assay. HeLa cells were infected with EPEC to follow actin-based pedestals formation by immunofluorescence where ~200 pedestals were counted for each experiment. Values are means ± SD of three independent experiments (error bars). Asterisks represent P-values (**, $P \leq 0.01$; ***, $P \leq 0.001$; Student's *t* test).

15 min of infection with *L. innocua*(InlB). Hip1R was found at the interface between EPEC and the actin pedestals throughout the infectious process.

We then used an siRNA-based approach to study the respective roles of Dab2, Myosin VI, and Hip1R in our infection models. The mean inhibition of protein expression was 80%, and no off-target effects on other components of the machinery were observed (Fig. S4). The depletion of Dab2, Myosin VI, or Hip1R efficiently inhibited *L. monocytogenes* internalization by the InlB pathway, whereas it had a milder but still significant effect the InlA-mediated internalization pathway (Fig. 5, a–c). This is in line with our previous observations of a compensatory role for caveolin that attenuates the clathrin knockdown phenotype in the InlA pathway (Bonazzi et al., 2008). Similarly, the formation of EPEC-induced actin pedestals was followed in cells depleted of Dab2, Myosin VI, and Hip1R, and infected with EPEC for 4, 5, and 6 h. Hip1R depletion efficiently inhibited the formation of EPEC-induced actin pedestals, whereas the knockdown of Dab2 had a milder effect (Fig. 5, a–c). In line with its lack of colocalization, the knockdown of Myosin VI had no effect on the formation of actin pedestals (Fig. 5 b).

Hierarchical organization of the clathrin–actin machinery

To dissect the respective roles of Dab2, CHC, CLC, Myosin VI, and Hip1R during infection, we observed the effects of single protein depletion on the other members of the machinery. We also used cytochalasin D to impair actin polymerization before infection. The knockdown of Dab2 had a clear effect on the recruitment of all members of the machinery including actin (Fig. 6 a). The depletion of CHC prevented binding of the CLC subunit and recruitment of Hip1R, and, as previously described (Veiga et al., 2007), blocked recruitment of actin. It also partially affected the recruitment of Myosin VI and Dab2 (Fig. 6 b), possibly affecting the latter by reducing coated pit stability. CLC depletion completely prevented recruitment of Hip1R and actin, while apparently having a partial effect on CHC, Dab2, and Myosin VI recruitment (Fig. 6 c). This partial effect is likely caused by decreased CHC stability in the absence of CLC, reducing CHC presence at the membrane. Despite its clear impact on *Listeria* internalization, Myosin VI depletion did not impair the recruitment of the other members of the clathrin–actin interaction machinery. These were even detected in higher quantities at the *Listeria* adhesion sites in the absence of Myosin VI, which reflects a lack of internalization (Fig. 6 d). The depletion of Myosin VI also did not affect protein recruitment at EPEC pedestals (Fig. 6 d). Hip1R depletion and cytochalasin D treatment had similar effects and both prevented the recruitment of actin and Hip1R at clathrin coats (Fig. 6, e and f). This latter effect likely reflects the strong influence that Hip1R and actin have on each other (Wilbur et al., 2008).

We next used the clathrin rescue assay to investigate the role of CHC phosphorylation in the organization of the clathrin-actin machinery. After treatment with siRNA, the ectopic expression of wt CHC-GFP efficiently rescued endogenous CHC depletion, and CHC-GFP was efficiently recruited at bacterial adhesion sites in all of the three infection models studied. Conversely, the Y1477, 1487F CHC-GFP mutant was not detected at sites of bacterial entry and adhesion. As previously observed, Dab2 localization was not significantly affected by the depletion of endogenous CHC (Figs. 6 and 7), and consequently, the overexpression of either wt or mutant CHC did not alter Dab2 recruitment at bacterial adhesion sites (Fig. 7). Notably, however, the recruitment of CLC, Hip1R, Myosin VI, and actin was restored to control levels in the case of the ectopic expression of wt CHC and not by the expression of the Y1477, 1487F mutant. Confirming our previous observations, Myosin VI was never recruited at EPEC-induced actin pedestals, regardless of the experimental condition (Fig. 7 c). Our data indicate that the tyrosine phosphorylation of CHC is required for the accumulation of clathrin coats at bacteria–cell interfaces, followed by the assembly of the clathrin–actin organizing machinery that mediates bacterial internalization or the formation of actin pedestals (Fig. 8).

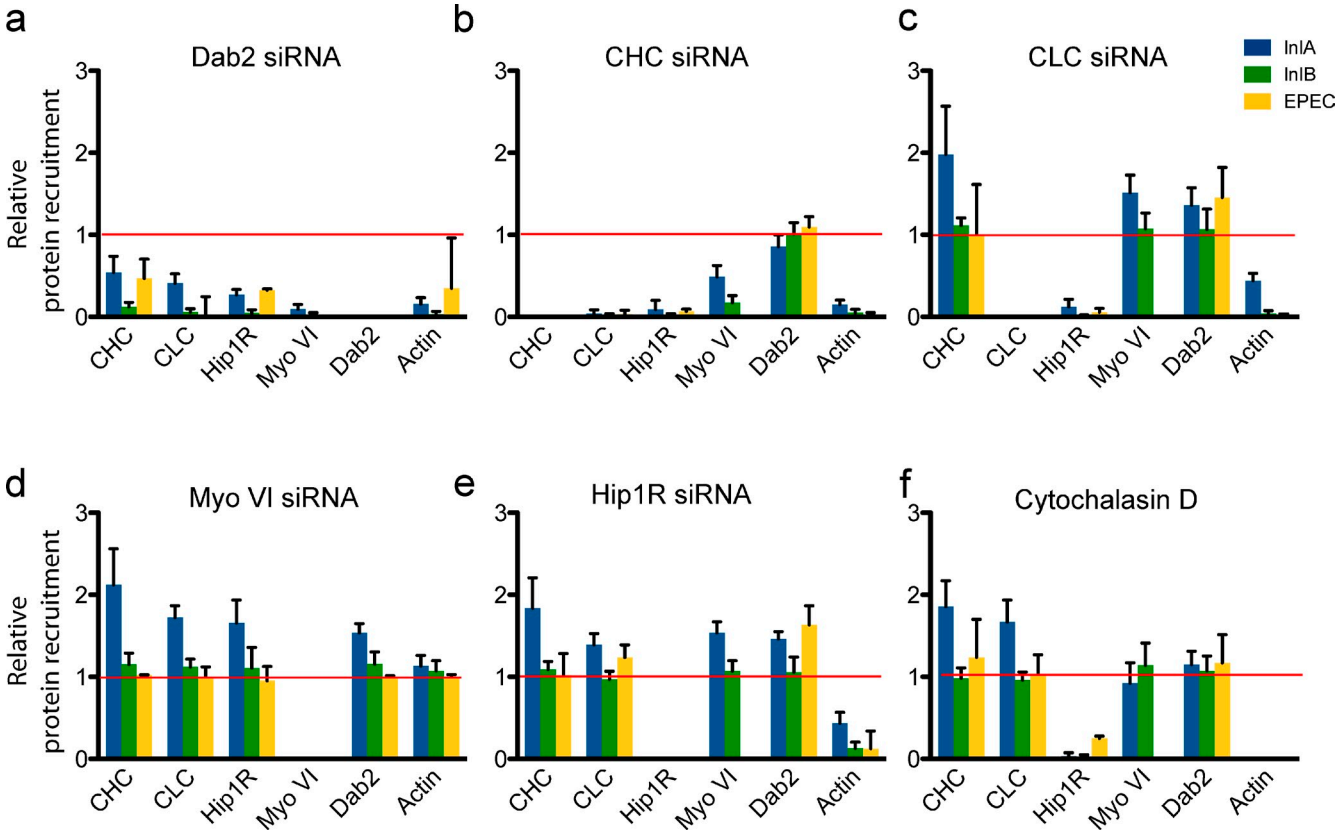

Figure 6. **Ordered recruitment of the clathrin-actin machinery established by siRNA treatment.** (a–f) Jeg3 and HeLa cells were transfected with siRNA targeted to either Dab2 (a), CHC (b), CLC (c), Myosin VI (d), or Hip1R (e); or incubated with cytochalasin D for 30 min (f). Cells were incubated with *L. innocua*(InlA), *L. innocua*(InlB), or EPEC, then fixed and processed by immunofluorescence. The frequency of recruitment of the different component of the clathrin/actin machinery at the bacterial adhesion sites was evaluated by fluorescence microscopy and normalized to that of control cells. Values are means (±SD) of three independent experiments where ~100 bacteria were counted for each condition. Red horizontal lines mark the control level of protein recruitment. Error bars indicate mean ± SD.

Discussion

Using three infection models, we provide here the first functional demonstration of a physiological role for the signaling-induced tyrosine phosphorylation of CHC. This posttranslational modification is needed for clathrin accumulation at the membrane as a prelude for actin cytoskeleton reorganization during bacterial adhesion and internalization. We also describe key components of the molecular machinery that orchestrates actin dynamics at clathrin coats, reinforcing the increasingly recognized link between clathrin and actin in mammalian cells (Kaksonen et al., 2006; Veiga et al., 2007; Cureton et al., 2009; Saffarian et al., 2009).

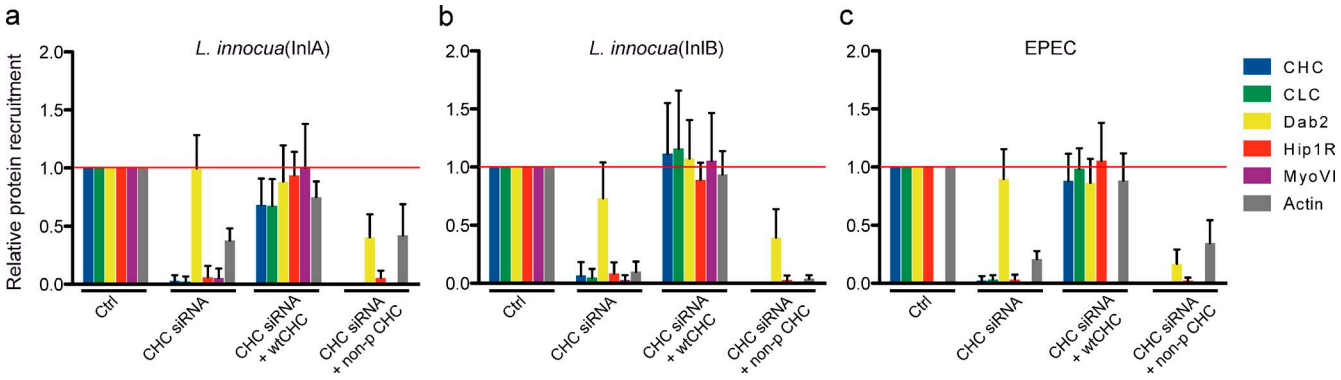

Figure 7. **CHC phosphorylation is required to assemble the clathrin-actin machinery.** (a–c) Jeg3 cells were transfected with a control siRNA or with a CHC-targeted siRNA, alone or in combination with the overexpression of wt CHC-GFP or the Y1477, 1487F mutant of CHC-GFP (non-p-CHC). Cells were then incubated with *L. innocua*(InlA), *L. innocua*(InlB), or EPEC, then fixed and processed by immunofluorescence. The frequency of recruitment of the different component of the clathrin–actin machinery at the bacterial adhesion sites was evaluated by fluorescence microscopy and normalized to that of control cells. Values are means ± SD of three independent experiments (error bars) where ~100 bacteria were counted for each condition.

Infection triggers the tyrosine phosphorylation of CHC

Clathrin-mediated internalization of cell surface receptors that signal through Src family kinases is accompanied by the tyrosine phosphorylation of CHC. Here we provide evidence for an essential role of this posttranslational modification during bacterial infections. By developing new tools for the study of CHC phosphorylation, we were able to show that the initial step of bacteria–host interactions triggers the phosphorylation of CHC, which occurs at tyrosines 1477 and 1487. In line with our previous observations (Sousa et al., 2007; Bonazzi et al., 2008), during InlA-mediated infections, CHC phosphorylation is mediated by Src family kinases. Indeed, the pretreatment of cells with the Src family kinase inhibitor PP1 before purified InlA incubation resulted in decreased phosphorylation of CHC. Our previous studies led to the hypothesis that the tyrosine phosphorylation of CHC might favor the accumulation of clathrin-coated pits so that they could be available for coordinated receptor uptake upon dephosphorylation and synchronized budding at the end of receptor signaling (Stoddart et al., 2002; Crotzer et al., 2004). In the case of bacterial interaction, the phosphorylated coated pits apparently serve as platforms for actin organization. However, completion of vesicle invagination may eventually serve an endocytic purpose later during infection, where clathrin-mediated endocytosis could play a role in vacuole maturation. Such an additional and more conventional role for clathrin at a later stage of infection would explain our earlier findings that dynamin and Hrs are also key proteins needed for successful infection (Veiga and Cossart, 2005). By analogy with the bacterial–host interactions we have observed, we speculate that phosphorylation-stabilized or "frozen" clathrin coated pits at the edge of immune cell signaling domains might also play a role in actin nucleation at the immunological synapse, whose organization is both clathrin and actin dependent (Calabia-Linares et al., 2011). Thus, phosphorylation of CHC may have a dual role of stabilizing clathrin as an actin-nucleating platform and providing a pool of coated pits that can be coordinately activated for endocytosis upon subsequent dephosphorylation. How tyrosine phosphorylation of CHC contributes to coated pit stability is not yet established. Because of its location on the proximal leg region, this modification could potentially block further addition of triskelia and freeze lattice growth through direct inhibition of regional interaction or recruitment of a blocking protein.

Defining components of clathrin–actin interaction during infection

The surprising observation that clathrin assembles into coated pits of conventional size at bacteria–host interfaces suggested that clathrin may serve a role during infection other than that of an endocytic protein. Here we demonstrate the sequential recruitment of Dab2, CHC, CLC, Hip1R, and Myosin VI to sites of host–pathogens interaction to orchestrate the recruitment of actin at sites of bacterial adhesion/internalization. Dab2 has been identified as the clathrin adaptor for the internalization of UPEC, where it functions in association with AP-2 (Eto et al., 2008), and a role for Dab2 in E-cadherin endocytosis has been reported during epithelial morphogenesis (Yang et al., 2007). Interestingly, AP-2 was never observed during *L. monocytogenes* entry, and its knockdown does not affect bacterial internalization (Veiga and Cossart, 2005). However, a role of Dab2 independent of AP-2 has been described (Maurer and Cooper, 2006). Furthermore, the NPXY consensus sequence recognized by Dab2 is not present in E-cadherin or Met, the host receptors for *L. monocytogenes*, which suggests that Dab2 must be associated with additional components that remain to be identified.

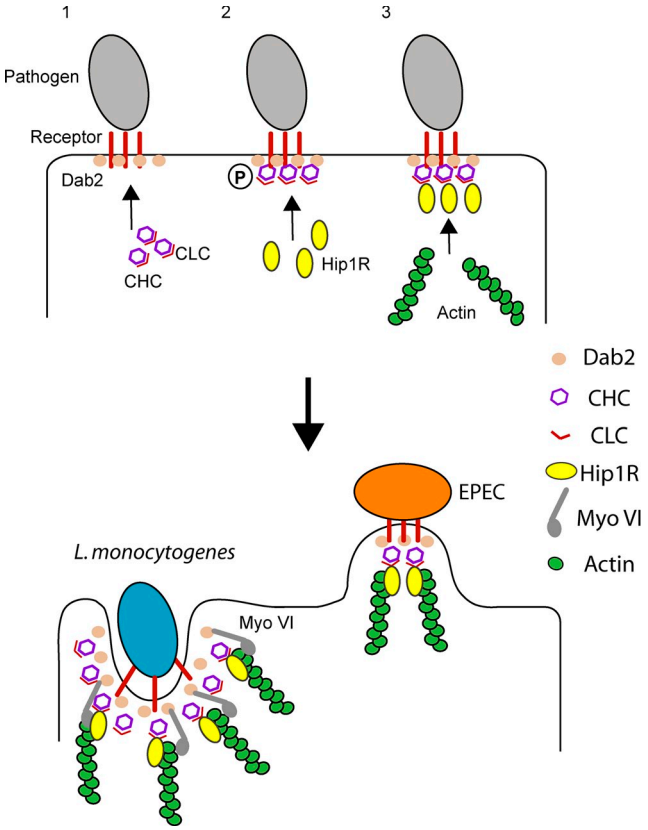

Figure 8. **Proposed model for the clathrin-actin machinery triggered by bacterial infection.** Bacteria activate host receptor downstream signaling, which results in the recruitment of the clathrin adaptor Dab2 and of the CHC–CLC complex. Clathrin coats are then stabilized by the tyrosine phosphorylation of CHC (P), followed by the sequential recruitment of Hip1R and actin. Myosin VI is also recruited in the case of invading bacteria, probably providing the pulling force for bacterial internalization, whereas it is excluded from EPEC-induced actin pedestals. CHC remains phosphorylated at the bacterial adhesion or internalization sites where clathrin and actin are colocalized.

CLC is a Hip protein interactor and a regulator of clathrin assembly (Chen and Brodsky, 2005; Legendre-Guillemin et al., 2005; Wilbur et al., 2010). Here we show that the interaction between CLC and Hip1R plays a key role in recruiting and organizing actin at clathrin coats. In our infection models, the knockdown of either CLC or Hip1R impedes the recruitment of actin at the bacterial adhesion sites, resulting in impaired bacterial internalization. Importantly, CLC depletion prevents Hip1R recruitment, which locates CLC upstream of Hip1R and demonstrates its essential role in the recruitment of Hip1R, hence actin, at clathrin coats.

Knockdown of the motor protein Myosin VI does not reduce the recruitment of all proteins of the clathrin–actin machinery at bacterial adhesion sites but prevents bacterial internalization. This identifies Myosin VI as the last component of such machinery that provides the pulling force for bacterial internalization, followed by the disassembly of clathrin coats. The absence of Myosin VI at pedestals likely reflects the fact that these are not internalization structures. Myosin VI recruitment at EPEC pedestals may be prevented by a bacterial type III effector, secreted upon adhesion to host cells.

In summary, by ectopic expression of a nonphosphorylatable mutant of CHC, we showed herein that the phosphorylation of CHC triggered by infection is the initiating event for the accumulation of clathrin coats at bacterial adhesion sites. These coats, via CLC–Hip1R interactions, in turn coordinate actin recruitment at bacterial–host adhesion sites (Fig. 8), leading either to internalization in conjunction with recruited Myosin VI or to pedestal formation. Thus, using bacterial infection models, we provide evidence that the clathrin–actin interaction mediated by CLC and Hip1R goes beyond its function in conventional coated vesicle endocytosis (Newpher and Lemmon, 2006; Boulant et al., 2011; Collins et al., 2011). We show here that, via the CLC–Hip1R interaction, the clathrin lattice can serve as a functional actin-organizing platform for uptake of structures that exceed the size limits of clathrin-coated vesicles and supports additional actin-based activities such as pedestal formation, unrelated to endocytosis. We further demonstrate that this novel function for clathrin in actin organization is dependent on CHC phosphorylation, thereby defining the functional consequence of CHC modification by Src family kinases, which are stimulated when signaling receptors are engaged during infection and initiation of endocytosis.

Materials and methods

Bacterial strains and cell lines

L. monocytogenes EGD (BUG 600) was grown in brain–heart infusion. *L. innocua* transformed with pRB474 harboring the *inlA* gene (BUG 1489) was grown in brain–heart infusion with 7 µg/ml chloramphenicol. *L. innocua* transformed with pP1-B3 harboring the inlB gene (BUG 1531) was grown in brain–heart infusion with 5 µg/ml erythromycin. EPEC strain JPN15 (BUG 2361) was grown in Luria-Bertani broth. Jeg3 cells (human epithelial placental cells ATCC n°: HTB-36) and HeLa cells (human cervix epithelial cells ATTC n°: CCL-2) were grown in MEM medium containing Glutamax, nonessential amino acids, sodium pyruvate, and 10% FBS.

Antibodies and reagents

PY20 anti-phosphotyrosine monoclonal antibody and anti-Hip1R polyclonal antibody were obtained from Millipore. Anti-Dab2 polyclonal antibody and anti-Myosin VI polyclonal antibody were obtained from Santa Cruz Biotechnology, Inc. Anti-actin monoclonal antibody was obtained from Sigma-Aldrich. Anti-CLC polyclonal antibody was produced as described previously (Acton et al., 1993), monoclonal antibodies against CHC (X22 for immunofluorescence and TD.1 for blotting were produced in our laboratory; Brodsky, 1985; Näthke et al., 1992), anti-InlA polyclonal antibody R302, anti-InlA monoclonal antibody L7.7, anti-InlB B4-6 monoclonal antibody, and anti–*L. innocua* polyclonal antibody R11 were produced in our laboratory. The 4G10 anti-phospho-tyrosine monoclonal antibody was obtained from the Bishop laboratory at University of California, San Francisco. Cytochalasin D was obtained from Sigma-Aldrich. To obtain the anti-pCHC antibody, rabbits were immunized with a phosphopeptide comprising CHC residues from 1473–1491, with phosphorylated tyrosines 1477 and 1487. The antibody was affinity purified by depletion with nonphosphorylated peptide 1473–1491, followed by positive purification with the immunizing peptide. The affinity-purified antibody was used directly for immunofluorescence. This affinity purified antibody was tested for peptide specificity by ELISA. The antibody at 1:1,000 dilution was incubated with purified peptides with two sites phosphorylated, one site phosphorylated, or nonphosphorylated in solution at the specified concentrations, then tested for binding to the double phospho-peptide using a secondary antibody coupled to horseradish peroxidase. For analysis by immunoblotting, the affinity-purified anti-pCHC antibody was further depleted by exposure to nonphosphorylated recombinant hub fragments immobilized on membrane as follows. 10 sets of 15 µg of purified hub were run on an SDS-PAGE gel and transferred to nitrocellulose membrane. Hub bands were cut out of the membrane and blocked with 5% BSA in PBS for 2 h. 100 µl of 9 µg/ml anti-pCHC was put onto the hub-loaded membrane for 1 h and pipetted every 10 min. After 1 h, the anti-pCHC was moved onto another-hub loaded membrane, and the process repeated. In total, the anti-pCHC was exposed to hub-loaded membranes 10 times. The depleted anti-pCHC was then tested by immunoblotting for binding to recombinant purified Hub protein (Liu et al., 1995) with or without exposure to purified Src kinase (Sigma-Aldrich).

Plasmids and siRNA sequences

siRNA targeting the CHC sequence 1, 5′-GGGAAUUCUUCGUACUCCATT-3′; and 2, 5′-GAUUAUCAAUUACCGUACATT-3′. The CLC sequence 1, 5′-AAAGACAGTTATGCAGCTATT-3′; and 2, 5′-AAGGAACCAGCGCCAGAGTGA-3′. Control siRNA sequences were obtained from Invitrogen. siRNA targeting the Hip1R sequence 1, 5′-CUCCGACAUGCUGUACUUCTT-3′; and 2, 5′-ACCGGAGAATCTCATTGAGATCTT-3′. The CHC sequence used for rescue analysis was 5′-GCAAUGAGCUGUUUGAAGA-3′. Control siRNA sequences were obtained from QIAGEN. siRNA targeting the Myosin VI sequence 1, 5′-GCUGGCAGUUCAUAGGAAUTT-3′; and 2, 5′-AUUCCUAUGAACUGCCAGCTT-3′. Control siRNA sequences were obtained from Eurogentec. siRNA targeting the Dab2 sequence 1, 5′-GCAAAGAUAUCCUGUUAGUTT-3′; and 2, 5′-GAACCAGCCUUCACCCUUUTT-3′. Control siRNA sequences were obtained from Thermo Fisher Scientific. For CHC rescue analysis, human CHC cDNA was made to be resistant to the CHC siRNA sequences used and inserted into a pcDNA3.1/Zeocin vector (Invitrogen) using the HindIII and NotI digestion sites. The siRNA-resistant human CHC cDNA was further mutated by site-directed mutagenesis using Quikchange II XL (Agilent Technologies) so that tyrosines 1477 and 1487 were mutated to code for phenylalanines. The resulting cDNA was then cloned into a pcDNA3.1/Zeocin vector using the HindIII and NotI digestion sites.

Transient transfections

For siRNA transfection, 2×10^5 cells/ml were mixed with siRNA and Lipofectamine RNAiMAX (Invitrogen) before plating according to manufacturer's instructions for reverse transfections. Cells were probed for siRNA efficacy 72 h after transfection by Western blotting. For CHC rescue experiments, 48 h after siRNA transfection, cells were transfected with the indicated clathrin constructs using Gene Juice according to manufacturer's instructions.

Fluorescence microscopy

Cells grown on glass coverslips were fixed in 4% paraformaldehyde at room temperature for 20 min, rinsed in PBS, and incubated for 20 min in blocking solution (0.5% BSA and 50 mM NH_4Cl in PBS, pH 7.4) supplemented with 0.05% saponin. Cells were then incubated for 30 min at room temperature with the appropriate primary antibodies diluted in blocking solution, washed five times in PBS, and incubated for 30 min at room temperature with Alexa Fluor–coupled secondary antibodies (Invitrogen). Where needed, Alexa Fluor–coupled phalloidin was added to the secondary antibodies to label the cell cytoskeleton. Cells were washed five times in PBS and mounted on microscope slides using Fluoromount mounting medium (Electron Microscopy Sciences). Preparations were analyzed using an epifluorescence microscope (Axiovert 135; Carl Zeiss) connected to a charge-coupled device camera (CoolSnap HQ; Photometrics) and operated by Metamorph software (Molecular Devices). Images were acquired using a 63× oil-immersion objective lens. Image analysis was performed using ImageJ (National Institutes of Health).

Transmission electron microscopy

Cells were grown on glass-bottomed Petri dishes and infected with either *L. innocua*(InlA) or *L. innocua*(InlB) at an MOI of 50. Cells were fixed in 2.5% glutaraldehyde in 0.1 M Hepes buffer, pH 7.2, overnight at 4°C, washed in 0.1 M Hepes buffer, postfixed for 1 h in 1% osmium + 1.5% K3[Fe(CN)6] in 0.1 M cacodylate buffer, pH 7.2, and washed in 0.1 M cacodylate buffer. Cells were then incubated for 1 h with 1% tannic acid

in 0.1 M cacodylate buffer and an additional 30 min with 1% osmium in 0.1 M cacodylate buffer. Cells were then dehydrated through a graded ethanol series and incubated overnight in a mixture of 50% pure ethanol and 50% EPON resin. Cells were then incubated in pure EPON and the resin was polymerized for 72 h at 65°C. For immunolabeling on thawed cryosections, cells were grown onto 100-mm Petri dishes and incubated with wt *L. monocytogenes* at an MOI of 50 for 20 min, then samples were fixed with a mixture of 2% paraformaldehyde and 0.1% glutaraldehyde in 0.1 M Sorensen's phosphate buffer. After quenching of free aldehyde groups, cells were scraped and pellets were embedded in 12% gelatin (TAAB). After hardening on ice, blocks of 1 mm^3 were cut and infiltrated overnight at 4°C with 2.1 M sucrose in 0.1 M phosphate buffer. Blocks were mounted on pins and frozen by plunging in liquid nitrogen. 60-nm sections were cut using a cryo-microtome (UC6/FC6; Leica) and picked up using a 1:1 mixture of 2% methylcellulose and 2.1 M sucrose. Sections were labeled at room temperature with the rabbit anti-CLC followed by protein A gold (Cell Microscopy Center) and observed with a transmission electron microscope (1010; Jeol) operated at 80 kV, equipped with a keenview camera (Olympus Soft imaging).

Infection-based assays

For the gentamicin survival assays, *L. monocytogenes* were grown at 37°C to an OD_{600} of 0.8–1.0. Before infection, bacteria were washed twice in PBS, diluted in DME, and incubated with either Jeg3 or HeLa cells (E-cadherin–expressing Jeg3 cells are mainly infected by the InlA pathway, and HeLa cells, which do not express E-cadherin, are mainly infected by the InlB pathway) at an MOI of 50. After 1 h of incubation at 37°C, cells were washed with complete culture medium and incubated for 2 h at 37°C in complete culture medium containing 10 µg/ml gentamicin. Cells were washed and lysed in 0.2% Triton X-100. The number of viable bacteria was assessed by titering on agar plates. For CHC rescue experiments, bacterial internalization was analyzed by double labeling bacteria before and after permeabilization (Veiga and Cossart, 2005), and the particle analysis plug-in of Image J was used to quantify internalized bacteria in CHC-GFP–expressing cells. For other assays, Jeg3 or HeLa cells were washed in serum-free culture medium and incubated with *L. innocua*(InlA) or *L. innocua*(InlB), respectively, at an MOI of 50. Cells were centrifuged for 2 min at 1,000 rpm and incubated at 37°C for the indicated times. Alternatively, HeLa cells were infected with EPEC at 37°C for the indicated times. At each time point, cells were fixed and processed for immunofluorescence. Protein recruitment and EPEC-induced actin pedestals formation were quantified by fluorescence microscopy where 100–200 events were observed for each condition. To hierarchically organize the components of the actin–clathrin machinery, values were then normalized versus the frequency of recruitment of a given protein in control conditions, and the fluctuations of such value when other members of the machinery are knocked down were plotted.

Transferrin uptake assay

Jeg3 cells were briefly washed in DME without serum and incubated in the same medium supplemented with 25 µg/ml Cy3-labeled transferrin and 20 mM Hepes for 30 min on ice. One sample was fixed immediately after that to measure the amount of surface-bound transferrin. A second sample was washed in PBS and subjected to a 4-min acid wash (500 mM NaCl, 0.5% acetic acid) to verify that all transferrin was extracellular. All remaining samples were incubated with either *L. innocua*(InlA), *L. innocua*(InlB), or EPEC as described above for 1 h at 37°C. Cells were then washed in PBS, subjected to the acid wash, and fixed and labeled with DAPI and with the anti–*L. innocua* antibody R11 where applicable. Cell-bound and/or intracellular transferrin was measured by fluorescence microscopy using ImageJ.

Immunoprecipitations

Immunoprecipitations were performed as described previously (Bonazzi et al., 2008). In brief, cells were treated as indicated, rinsed in pre-chilled PBS at 4°C, and incubated in 500 ml of lysis buffer (1% NP-40, 20 mM Tris, pH 8.0, 150 mM NaCl, 10% glycerol, 20 mM NaF, 5 mM Na_3VO_4, and complete protease inhibitors cocktail; Roche). Cells were then scraped and collected in 1.5 ml Eppendorf tubes and further incubated in the lysis buffer for 15 min at 4°C on a spinning wheel. Lysates were centrifuged for 15 min at 4°C at maximum speed and the supernatants were incubated for 1 h at 4°C with protein A–Sepharose beads to eliminate unspecific binding of proteins to beads. Lysates were then centrifuged to eliminate beads and incubated overnight at 4°C on a spinning wheel with the anti-CHC antibody. Protein A beads were added to samples and incubated at 4°C for 3 h. Samples were then centrifuged for 2 min at 4°C at maximum speed, and the supernatants were discarded. Beads were then washed in lysis buffer and resuspended in Laemmli loading buffer. Samples were then loaded on an 8% poly-acrylamide gel and blotted for protein analysis.

Mass spectrometry

Src kinase was incubated with recombinant CHC (Hub) followed by digestion with trypsin and collection of peptide masses by matrix-assisted laser desorption/ionization (MALDI) time of flight (TOF). Peptides masses in the mass spectrum were manually matched to expected peptide masses, and identification of phospho-peptides was determined by the presence of two peptides with an 80-D mass difference. The peptide sequence and the presence of phospho-tyrosine were confirmed by MALDI TOF/TOF analysis.

Online supplemental material

Fig. S1 shows bacterial infection and incubation with bacterial surface proteins involved in *L. monocytogenes* internalization phosphorylate CHC. When cells are incubated with the *L. monocytogenes* surface protein InlA, CHC phosphorylation is dependent on Src family kinases. Fig. S2 shows that EGF treatment of cells promotes the accumulation of phosphorylated CHC at the plasma membrane. Fig. S3 shows that bacterial infection does not affect the clathrin-mediated internalization of transferrin. Fig. S4 shows the efficiency and specificity of the siRNA interference treatments used in this study. Online supplemental material is available at http://www.jcb.org/cgi/content/full/jcb.201105152/DC1.

This work was supported by Institut Pasteur, Institut National de la Santé et de la Recherche Médicale, Institut National de la Recherche Agronomique, European Research Council (advanced grant 233348) to P. Cossart, and grant GM038093 from the National Institutes of Health and grant 15IB-0035 from the California Breast Cancer Research Program to F.M. Brodsky. M. Bonazzi is supported by the Pasteur Roux Fellowship. P. Cossart is an international research scholar of the Howard Hughes Medical Institute.

Submitted: 26 May 2011
Accepted: 3 October 2011

References

Acton, S.L., D.H. Wong, P. Parham, F.M. Brodsky, and A.P. Jackson. 1993. Alteration of clathrin light chain expression by transfection and gene disruption. *Mol. Biol. Cell.* 4:647–660.

Bonazzi, M., E. Veiga, J. Pizarro-Cerdá, and P. Cossart. 2008. Successive post-translational modifications of E-cadherin are required for InlA-mediated internalization of *Listeria monocytogenes*. *Cell. Microbiol.* 10:2208–2222. http://dx.doi.org/10.1111/j.1462-5822.2008.01200.x

Boulant, S., C. Kural, J.-C. Zeeh, F. Ubelmann, and T. Kirchhausen. 2011. Actin dynamics counteract membrane tension during clathrin-mediated endocytosis. *Nat. Cell Biol.* 13:1124–1131. http://dx.doi.org/10.1038/ncb2307

Brodsky, F.M. 1985. Clathrin structure characterized with monoclonal antibodies. I. Analysis of multiple antigenic sites. *J. Cell Biol.* 101:2047–2054. http://dx.doi.org/10.1083/jcb.101.6.2047

Brodsky, F.M., C.Y. Chen, C. Knuehl, M.C. Towler, and D.E. Wakeham. 2001. Biological basket weaving: formation and function of clathrin-coated vesicles. *Annu. Rev. Cell Dev. Biol.* 17:517–568. http://dx.doi.org/10.1146/annurev.cellbio.17.1.517

Buss, F., S.D. Arden, M. Lindsay, J.P. Luzio, and J. Kendrick-Jones. 2001a. Myosin VI isoform localized to clathrin-coated vesicles with a role in clathrin-mediated endocytosis. *EMBO J.* 20:3676–3684. http://dx.doi.org/10.1093/emboj/20.14.3676

Buss, F., J.P. Luzio, and J. Kendrick-Jones. 2001b. Myosin VI, a new force in clathrin mediated endocytosis. *FEBS Lett.* 508:295–299. http://dx.doi.org/10.1016/S0014-5793(01)03065-4

Calabia-Linares, C., J. Robles-Valero, H. de la Fuente, M. Perez-Martinez, N. Martín-Cofreces, M. Alfonso-Pérez, C. Gutierrez-Vázquez, M. Mittelbrunn, S. Ibiza, F.R. Urbano-Olmos, et al. 2011. Endosomal clathrin drives actin accumulation at the immunological synapse. *J. Cell Sci.* 124:820–830. http://dx.doi.org/10.1242/jcs.078832

Carreno, S., A.E. Engqvist-Goldstein, C.X. Zhang, K.L. McDonald, and D.G. Drubin. 2004. Actin dynamics coupled to clathrin-coated vesicle formation at the trans-Golgi network. *J. Cell Biol.* 165:781–788. http://dx.doi.org/10.1083/jcb.200403120

Chan, Y.G.Y., M.M. Cardwell, T.M. Hermanas, T. Uchiyama, and J.J. Martinez. 2009. Rickettsial outer-membrane protein B (rOmpB) mediates bacterial invasion through Ku70 in an actin, c-Cbl, clathrin and caveolin 2-dependent manner. *Cell. Microbiol.* 11:629–644. http://dx.doi.org/10.1111/j.1462-5822.2008.01279.x

Chen, C.Y., and F.M. Brodsky. 2005. Huntingtin-interacting protein 1 (Hip1) and Hip1-related protein (Hip1R) bind the conserved sequence of clathrin light chains and thereby influence clathrin assembly in vitro and actin distribution in vivo. *J. Biol. Chem.* 280:6109–6117. http://dx.doi.org/10.1074/jbc.M408454200

Collins, A., A. Warrington, K.A. Taylor, and T. Svitkina. 2011. Structural organization of the actin cytoskeleton at sites of clathrin-mediated endocytosis. *Curr. Biol.* 21:1167–1175. http://dx.doi.org/10.1016/j.cub.2011.05.048

Crotzer, V.L., A.S. Mabardy, A. Weiss, and F.M. Brodsky. 2004. T cell receptor engagement leads to phosphorylation of clathrin heavy chain during receptor internalization. *J. Exp. Med.* 199:981–991. http://dx.doi.org/10.1084/jem.20031105

Cureton, D.K., R.H. Massol, S. Saffarian, T.L. Kirchhausen, and S.P.J. Whelan. 2009. Vesicular stomatitis virus enters cells through vesicles incompletely coated with clathrin that depend upon actin for internalization. *PLoS Pathog.* 5:e1000394. http://dx.doi.org/10.1371/journal.ppat.1000394

Engqvist-Goldstein, A.E., R.A. Warren, M.M. Kessels, J.H. Keen, J. Heuser, and D.G. Drubin. 2001. The actin-binding protein Hip1R associates with clathrin during early stages of endocytosis and promotes clathrin assembly in vitro. *J. Cell Biol.* 154:1209–1223. http://dx.doi.org/10.1083/jcb.200106089

Engqvist-Goldstein, A.E.Y., C.X. Zhang, S. Carreno, C. Barroso, J.E. Heuser, and D.G. Drubin. 2004. RNAi-mediated Hip1R silencing results in stable association between the endocytic machinery and the actin assembly machinery. *Mol. Biol. Cell*. 15:1666–1679. http://dx.doi.org/10.1091/mbc.E03-09-0639

Eto, D.S., H.B. Gordon, B.K. Dhakal, T.A. Jones, and M.A. Mulvey. 2008. Clathrin, AP-2, and the NPXY-binding subset of alternate endocytic adaptors facilitate FimH-mediated bacterial invasion of host cells. *Cell. Microbiol.* 10:2553–2567. http://dx.doi.org/10.1111/j.1462-5822.2008.01229.x

Ferguson, S.M., A. Raimondi, S. Paradise, H. Shen, K. Mesaki, A. Ferguson, O. Destaing, G. Ko, J. Takasaki, O. Cremona, et al. 2009. Coordinated actions of actin and BAR proteins upstream of dynamin at endocytic clathrin-coated pits. *Dev. Cell*. 17:811–822. (published erratum appears in *Dev. Cell*. 2010. 18:332) http://dx.doi.org/10.1016/j.devcel.2009.11.005

Hyman, T., M. Shmuel, and Y. Altschuler. 2006. Actin is required for endocytosis at the apical surface of Madin-Darby canine kidney cells where ARF6 and clathrin regulate the actin cytoskeleton. *Mol. Biol. Cell*. 17:427–437. http://dx.doi.org/10.1091/mbc.E05-05-0420

Inoue, A., O. Sato, K. Homma, and M. Ikebe. 2002. DOC-2/DAB2 is the binding partner of myosin VI. *Biochem. Biophys. Res. Commun.* 292:300–307. http://dx.doi.org/10.1006/bbrc.2002.6636

Jonquières, R., H. Bierne, F. Fiedler, P. Gounon, and P. Cossart. 1999. Interaction between the protein InlB of *Listeria monocytogenes* and lipoteichoic acid: a novel mechanism of protein association at the surface of gram-positive bacteria. *Mol. Microbiol.* 34:902–914. http://dx.doi.org/10.1046/j.1365-2958.1999.01652.x

Kaksonen, M., C.P. Toret, and D.G. Drubin. 2006. Harnessing actin dynamics for clathrin-mediated endocytosis. *Nat. Rev. Mol. Cell Biol.* 7:404–414. http://dx.doi.org/10.1038/nrm1940

Le Clainche, C., B.S. Pauly, C.X. Zhang, A.E.Y. Engqvist-Goldstein, K. Cunningham, and D.G. Drubin. 2007. A Hip1R-cortactin complex negatively regulates actin assembly associated with endocytosis. *EMBO J.* 26:1199–1210. http://dx.doi.org/10.1038/sj.emboj.7601576

Legendre-Guillemin, V., M. Metzler, J.F. Lemaire, J. Philie, L. Gan, M.R. Hayden, and P.S. McPherson. 2005. Huntingtin interacting protein 1 (HIP1) regulates clathrin assembly through direct binding to the regulatory region of the clathrin light chain. *J. Biol. Chem.* 280:6101–6108. http://dx.doi.org/10.1074/jbc.M408430200

Liu, S.H., M.L. Wong, C.S. Craik, and F.M. Brodsky. 1995. Regulation of clathrin assembly and trimerization defined using recombinant triskelion hubs. *Cell*. 83:257–267. http://dx.doi.org/10.1016/0092-8674(95)90167-1

Maurer, M.E., and J.A. Cooper. 2006. The adaptor protein Dab2 sorts LDL receptors into coated pits independently of AP-2 and ARH. *J. Cell Sci.* 119:4235–4246. http://dx.doi.org/10.1242/jcs.03217

Mengaud, J., H. Ohayon, P. Gounon, R.-M. Mege, and P. Cossart. 1996. E-cadherin is the receptor for internalin, a surface protein required for entry of *L. monocytogenes* into epithelial cells. *Cell*. 84:923–932. http://dx.doi.org/10.1016/S0092-8674(00)81070-3

Merrifield, C.J., M.E. Feldman, L. Wan, and W. Almers. 2002. Imaging actin and dynamin recruitment during invagination of single clathrin-coated pits. *Nat. Cell Biol.* 4:691–698. http://dx.doi.org/10.1038/ncb837

Mettlen, M., D. Loerke, D. Yarar, G. Danuser, and S.L. Schmid. 2010. Cargo- and adaptor-specific mechanisms regulate clathrin-mediated endocytosis. *J. Cell Biol.* 188:919–933. http://dx.doi.org/10.1083/jcb.200908078

Moreno-Ruiz, E., M. Galán-Díez, W. Zhu, E. Fernández-Ruiz, C. d'Enfert, S.G. Filler, P. Cossart, and E. Veiga. 2009. *Candida albicans* internalization by host cells is mediated by a clathrin-dependent mechanism. *Cell. Microbiol.* 11:1179–1189. http://dx.doi.org/10.1111/j.1462-5822.2009.01319.x

Morris, S.M., S.D. Arden, R.C. Roberts, J. Kendrick-Jones, J.A. Cooper, J.P. Luzio, and F. Buss. 2002. Myosin VI binds to and localises with Dab2, potentially linking receptor-mediated endocytosis and the actin cytoskeleton. *Traffic*. 3:331–341. http://dx.doi.org/10.1034/j.1600-0854.2002.30503.x

Näthke, I.S., J. Heuser, A. Lupas, J. Stock, C.W. Turck, and F.M. Brodsky. 1992. Folding and trimerization of clathrin subunits at the triskelion hub. *Cell*. 68:899–910. http://dx.doi.org/10.1016/0092-8674(92)90033-9

Newpher, T.M., and S.K. Lemmon. 2006. Clathrin is important for normal actin dynamics and progression of Sla2p-containing patches during endocytosis in yeast. *Traffic*. 7:574–588. http://dx.doi.org/10.1111/j.1600-0854.2006.00410.x

Pizarro-Cerdá, J., B. Payrastre, Y.J. Wang, E. Veiga, H.L. Yin, and P. Cossart. 2007. Type II phosphatidylinositol 4-kinases promote *Listeria monocytogenes* entry into target cells. *Cell. Microbiol.* 9:2381–2390. http://dx.doi.org/10.1111/j.1462-5822.2007.00967.x

Pizarro-Cerdá, J., M. Bonazzi, and P. Cossart. 2010. Clathrin-mediated endocytosis: what works for small, also works for big. *Bioessays*. 32:496–504. http://dx.doi.org/10.1002/bies.200900172

Popoff, V., G.A. Mardones, S.K. Bai, V.R. Chambon, D.L. Tenza, P.V. Burgos, A. Shi, P. Benaroch, S. Urbé, C. Lamaze, et al. 2009. Analysis of articulation between clathrin and retromer in retrograde sorting on early endosomes. *Traffic*. 10:1868–1880. http://dx.doi.org/10.1111/j.1600-0854.2009.00993.x

Raiborg, C., and H. Stenmark. 2009. The ESCRT machinery in endosomal sorting of ubiquitylated membrane proteins. *Nature*. 458:445–452. http://dx.doi.org/10.1038/nature07961

Saffarian, S., E. Cocucci, and T. Kirchhausen. 2009. Distinct dynamics of endocytic clathrin-coated pits and coated plaques. *PLoS Biol.* 7:e1000191. http://dx.doi.org/10.1371/journal.pbio.1000191

Sousa, S., D. Cabanes, L. Bougnères, M. Lecuit, P. Sansonetti, G. Tran-Van-Nhieu, and P. Cossart. 2007. Src, cortactin and Arp2/3 complex are required for E-cadherin-mediated internalization of *Listeria* into cells. *Cell. Microbiol.* 9:2629–2643. http://dx.doi.org/10.1111/j.1462-5822.2007.00984.x

Stoddart, A., M.L. Dykstra, B.K. Brown, W. Song, S.K. Pierce, and F.M. Brodsky. 2002. Lipid rafts unite signaling cascades with clathrin to regulate BCR internalization. *Immunity*. 17:451–462. http://dx.doi.org/10.1016/S1074-7613(02)00416-8

Veiga, E., and P. Cossart. 2005. Listeria hijacks the clathrin-dependent endocytic machinery to invade mammalian cells. *Nat. Cell Biol.* 7:894–900. http://dx.doi.org/10.1038/ncb1292

Veiga, E., J.A. Guttman, M. Bonazzi, E. Boucrot, A. Toledo-Arana, A.E. Lin, J. Enninga, J. Pizarro-Cerdá, B.B. Finlay, T. Kirchhausen, and P. Cossart. 2007. Invasive and adherent bacterial pathogens co-opt host clathrin for infection. *Cell Host Microbe*. 2:340–351. http://dx.doi.org/10.1016/j.chom.2007.10.001

Wilbur, J.D., C.Y. Chen, V. Manalo, P.K. Hwang, R.J. Fletterick, and F.M. Brodsky. 2008. Actin binding by Hip1 (huntingtin-interacting protein 1) and Hip1R (Hip1-related protein) is regulated by clathrin light chain. *J. Biol. Chem.* 283:32870–32879. http://dx.doi.org/10.1074/jbc.M802863200

Wilbur, J.D., P.K. Hwang, J.A. Ybe, M. Lane, B.D. Sellers, M.P. Jacobson, R.J. Fletterick, and F.M. Brodsky. 2010. Conformation switching of clathrin light chain regulates clathrin lattice assembly. *Dev. Cell*. 18:854–861. http://dx.doi.org/10.1016/j.devcel.2010.04.007

Wilde, A., E.C. Beattie, L. Lem, D.A. Riethof, S.H. Liu, W.C. Mobley, P. Soriano, and F.M. Brodsky. 1999. EGF receptor signaling stimulates SRC kinase phosphorylation of clathrin, influencing clathrin redistribution and EGF uptake. *Cell*. 96:677–687. http://dx.doi.org/10.1016/S0092-8674(00)80578-4

Wong, A.R.C., J.S. Pearson, M.D. Bright, D. Munera, K.S. Robinson, S.F. Lee, G. Frankel, and E.L. Hartland. 2011. Enteropathogenic and enterohaemorrhagic *Escherichia coli*: even more subversive elements. *Mol. Microbiol.* 80:1420–1438. http://dx.doi.org/10.1111/j.1365-2958.2011.07661.x

Yang, D.H., K.Q. Cai, I.H. Roland, E.R. Smith, and X.X. Xu. 2007. Disabled-2 is an epithelial surface positioning gene. *J. Biol. Chem.* 282:13114–13122. http://dx.doi.org/10.1074/jbc.M611356200

Yarar, D., C.M. Waterman-Storer, and S.L. Schmid. 2005. A dynamic actin cytoskeleton functions at multiple stages of clathrin-mediated endocytosis. *Mol. Biol. Cell*. 16:964–975. http://dx.doi.org/10.1091/mbc.E04-09-0774